Calhoun

Institutional Archive of the Naval Postgraduate School

Calhoun: The NPS Institutional Archive

Faculty and Researcher Publications   Faculty and Researcher Publications Collection

Atomic and molecular ejection from ion-bombarded reacted single-crystal surfaces: oxygen on copper (100)

Garrison, B.J.

American Physical Society

Atomic and molecular ejection from ion-bombarded reacted single-crystal surfaces. Oxygen on copper(100)

B. J. Garrison*

Department of Chemistry, University of California, Berkeley, California 94720

N. Winograd

Department of Chemistry, Purdue University, West Lafayette, Indiana 47907

D. E. Harrison, Jr.

Department of Physics and Chemistry, Naval Postgraduate School, Monterey, California 93940

The trajectories of atomic and molecular species ejected from an ion-bombarded reacted single-crystal surface have been calculated using classical dynamics. As a model system, oxygen has been adsorbed in various coverages and site geometries on the (100) face of a copper surface, which is then bombarded by 600-eV Ar^+ ions at normal incidence. The oxygen atoms have been placed at near zero (single-atom adsorption), $p(2 \times 2)$ and $c(2 \times 2)$ coverages in an A-top site, a fourfold bridge site, and a twofold bridge site. From the calculated positions and momenta of the ejected adsorbate and substrate atoms, we have identified the important ejection mechanisms, determined relative yields, and determined the factors that influence multimer formation. Of mechanistic interest is that oxygen is most often ejected by collisions with an adjacent copper atom rather than by collisions with the copper atom directly beneath it. The calculations show that multimers of the types Cu_2, CuO, O_2, Cu_3, Cu_2O, CuO_2, O_3, and several tetramers and pentamers can be expected to form. These multimers establish their identity over the surface and do not directly eject as a molecular entity. The influence of site geometry on multimer yields is discussed in detail. In general, the bridge sites have higher multimer yields than the A-top site. The surface coverage also exerts a systematic influence on the types of clusters that are observed. For example, molecules like O_2 and CuO_2 are not likely to be ejected from a $p(2 \times 2)$ surface due to a large O-O separation distance.

I. INTRODUCTION

The characterization of atoms and molecules adsorbed on surfaces has been the subject of numerous investigations over the past few years. Several experiments have indicated that ion beams of kinetic energy 0.5–5 keV are valuable probes for study of these systems since either the secondary ejected particles[1-4] or the energy of the reflected primary ion[5] can be determined with high sensitivity to submonolayer amounts of material. Of special interest is the application of secondary-ion mass spectrometry (SIMS) to the elucidation of the chemistry and structure of adsorbates on metals.[1-4,6,7] Such studies are especially valuable when the primary-ion dose is kept less than the total number of surface atoms to minimize chemical damage by the primary-ion beam. With this technique, it is clear that the different adsorption states of oxygen on several metals can be empirically distinguished[2,4] and that the onset of bulk oxide formation can be determined by enhanced positive-ion intensities of larger metal-oxide clusters.[2] It has also been proposed that for CO, dissociative adsorption can be distinguished from molecular adsorption.[7] Of particular note is the proposal that the site geometry of CO on nickel can be determined from the

Ni_2CO^+ to $NiCO^+$ intensity ratio.[3]

Only a few attempts have been made to develop a comprehensive theory for the ejection of atoms and molecules from reacted surfaces. The specific case of low-energy He^+ ion bombardment of nitrogen adsorbed on tungsten has been treated using the binary collision approximation (BCA). In this case it was postulated that the nitrogen atoms could only be desorbed by direct collisions with the primary ion.[8] Several desorption cross sections for atoms on ion bombarded surfaces have also been calculated using the BCA via the computer program MORLAY,[9] but agreement with experiment has been poor.

An atomistic understanding of these processes depends on our ability to calculate the dynamics of a large number of atoms which surround the impact site, after they have received the initial momentum of the primary ion. For the SIMS experiment the ionization mechanism of the emitted atom or molecule must also be known, since the ionization probability largely determines the intensity of the observed species. Several recent ideas have been advanced to explain the ionization process,[10,11] although none have addressed the problem of molecular-ion ejection. It would seem that a detailed knowledge of atomic trajectories subsequent to the

ion bombardment is a necessary first step in composing atomistically based ionization theories.

Using classical dynamics to model the dissipation of momentum of the primary ion, advances have been made in our knowledge about ion bombardment of metal surfaces in this energy regime.[12-15] Although this method has been successful in predicting a wide range of experimental observables, the question remains as to how much of this information is extendable to reacted systems. At the present time, except for the few specific cases sited above, we are unaware of any discussion concerning the mechanisms by which adsorbed atoms may leave the surface. It is not known, for example, whether the metal-oxygen molecular clusters observed in SIMS form from contiguous surface atoms or whether rearrangement is possible during ejection. The influence of surface coverage and adsorption site geometry on ejection mechanisms and yields of both adsorbate and substrate is also unknown.

In this paper we extend our calculations concerning the dynamics of atoms in an ion-bombarded metal to include adsorbed atoms. As a model system we have chosen to adsorb oxygen atoms in various coverages and site geometries on the (100) face of a copper surface. From the calculated positions and momenta of the ejected adsorbate and substrate atoms, we have identified the important ejection mechanisms, determined relative yields (defined as the number of ejected particles per number of incident ions), and determined the factors which influence multimer formation. Of mechanistic interest is that oxygen is most often found to be ejected by collisions with adjacent copper atoms rather than by collision with the copper atom directly beneath it. The calculations have also shown that a variety of clusters are ejected from the solid including Cu_2, CuO, and O_2 dimers, Cu_3, Cu_2O, CuO_2, and O_3 trimers, as well as several tetramers and pentamers. As in the case of clean metals[13,14] these multimers establish their identity over the surface and do not directly eject as a molecular entity. In addition, we also discuss the influence of site geometry on multimer yields. In general, we have found that the bridge sites have higher multimer yields than the A-top site. We have also noted that the surface coverage exerts a systematic influence on the types of clusters that are observed. For example, molecules like O_2 and CuO_2 are not ejected from low coverage configurations due to the large O-O distances.

II. DESCRIPTION OF THE CALCULATION

The dynamics of the bombarding ion, the metal substrate, and the oxygen adsorbate have been modeled classically. We have approximated the metal-oxygen system by a microcrystallite with oxygen atoms placed in various sites on the surface. The positions and momenta have been determined in time by integrating Hamilton's equations of motion using a scheme described previously.[16-18] To represent the interaction potential, we have used a sum of pair potentials between all the atoms. The pair-potential functions for the atoms in bulk phase are composed of three parts, a repulsive Born-Mayer function for small internuclear separations, an attractive Morse potential at long range, and a cubic spline to connect the two. The composite pair potential V_{ij} between the ith and jth atoms separated by a distance R is given by

$$V_{ij} = Ae^{-BR}, \quad R < R_a, \tag{1}$$

$$V_{ij} = C_0 + C_1R + C_2R^2 + C_3R^3, \quad R_a \leq R \leq R_b, \tag{2}$$

$$V_{ij} = D_e e^{-\beta(R-R_e)}(e^{-\beta(R-R_e)} - 2), \quad R_b < R < R_c, \tag{3}$$

$$V_{ij} = 0, \quad R \geq R_c. \tag{4}$$

The interaction of Ar^+ with the other species is represented by a purely repulsive function

$$V_{ij} = Ae^{-BR}, \quad R < R_a, \tag{5}$$

$$V_{ij} = 0, \quad R \geq R_a. \tag{6}$$

Exact potential surfaces, or for that matter pair potentials which represent the oxygen-metal interaction, are presently unavailable. To avoid the ambiguity of adjusting the potential parameters to a particular set of desired properties, we have treated the adsorbate using a pair potential having the same form as the substrate potential, but with the mass of oxygen. Our studies clearly show, however, that the exact form of the adsorbate potential is not of great importance. The atomic placement is the overriding factor in determining ejection mechanisms and relative yields for different configurations. We therefore believe our potential gives realistic insight into understanding the basic processes involved during the ion bombardment event. All of the potential parameters are given in Table I.

The binding energy E_b of the adsorbate has been altered over a reasonable range for chemisorbed species as shown in Table II. Its value is calculated as the sum of the pairwise interactions of the oxygen atom with the rest of the atoms as determined by Eq. (3). We used the various D_e values shown in Table I with the oxygen atom in its equilibrium configurations.

The oxygen coverages used in this study were low enough so that oxygen-oxygen interactions were minimal when the atoms were in their initial configurations. During a trajectory, we approximated the oxygen-oxygen collisional interactions with the

TABLE I. Potential parameters.

Bulk	A (keV)	B (Å⁻¹)	C_0 (eV)	C_1[a] (eV/Å)	C_2[a] (eV/Å²)	C_3[a] (eV/Å³)	D_e (eV)	β (Å⁻¹)	R_e (Å)	R_a (Å)	R_b (Å)	R_c (Å)
Cu–Cu	22.564	5.088	588	−880	444	−74.8	0.48	1.405	2.628	1.500	1.988	4.338
O–O	22.564	5.088	588	−880	444	−74.8	0.48	1.405	2.628	1.500	1.988	3.525[b]
Cu–O	22.564	5.088	92.8	−109	42.2	− 5.50	0.18	1.405	2.628	1.898	2.440	4.338
			94.3	−110	42.5	− 5.49	0.27	1.405	2.628	1.880	2.404	4.338
			588	−880	444	−74.8	0.48	1.405	2.628	1.500[c]	1.988[c]	4.338
			165.0	−212	92.7	−13.6	0.73	1.405	2.628	1.808	2.169	4.338
Ar⁺–Cu	71.303	4.593	•••	•••	•••	•••	•••	•••	•••	2.556	•••	•••
Ar⁺–O	22.564	5.088	•••	•••	•••	•••	•••	•••	•••	2.556	•••	•••
Gas Phase												
Cu₂	•••	•••	•••	•••	•••	•••	2.05	1.41	2.22	•••	•••	•••
O₂	•••	•••	•••	•••	•••	•••	5.12	2.67	1.21	•••	•••	•••
CuO	•••	•••	•••	•••	•••	•••	2.72	1.96	1.73	•••	•••	•••
O₂⁻	•••	•••	•••	•••	•••	•••	4.07	2.11	1.31	•••	•••	•••
O₂⁺	•••	•••	•••	•••	•••	•••	6.48	2.87	1.12	•••	•••	•••

[a] Coefficients in the cubic spline are determined by smoothly connecting the Born-Mayer potential to Morse potential.

[b] O–O cutoff is smaller than the Cu–Cu and Cu–O to keep the oxygens from interacting on the surface. If the range (R_c) is larger the oxygen overlayer is artifically stabilized.

[c] Values of R_a and R_b for D_e = 0.48 eV are the same as for Cu–Cu. A slightly different procedure was used to determine the other R_a's and R_b's, thus they do not exhibit continuous variation.

bulk-metal potential, but with an oxygen mass.

Three different adsorption site geometries have been considered: the A-top site where the oxygen is directly above a copper atom; the four-fold bridge site where the oxygen is equidistant from four surface copper atoms; and a two-fold bridge site where the oxygen is equidistant from two surface copper atoms. These positions are shown schematically in Fig. 1. For each of these sites the oxygen is placed at an equilibrium height above the surface layer of 2.55, 2.13, and 1.74 Å for the A top, two-fold bridge, and four-fold bridge sites, respectively. Note that the four-fold oxygen is closest to the surface while the A-top oxygen is furthest away.

The calculations have been performed for three different coverages of oxygen on the copper (100) orientation. To carefully determine the important ejection mechanisms for adsorbed oxygen, we first placed a single atom in an A-top site on the microcrystallite surface. This configuration approximates the zero coverage limit in that the oxygen-oxygen scattering mechanisms can not occur. If the oxygen is located on top of the center copper atom of the microcrystallite, the impact zone of irreducible surface symmetry grows to $\frac{1}{8}$ of the entire surface. We can maintain the same relative positions of the impact points to the oxygen atom by using the impact zone of the clean metal, and independently placing the oxygen atom on each of the surface copper atoms. These two methods require the same number of impact points to generate equivalent information. In the first case the points cover $\frac{1}{8}$ of the crystallite surface, while in the second case the impact points are duplicated in the smaller clean metal zone as the oxygen is consecu-

TABLE II. Calculated surface binding energies.

D_e (eV) [a]	A top	E_b (eV) Twofold bridge	Fourfold bridge
0.18	0.50	0.74	0.76
0.27	0.74	1.10	1.12
0.48	1.32	1.95	2.01
0.73	2.00	2.96	3.04

[a] Remaining potential parameters are given in Table I.

(a) CLEAN   (b) A-TOP

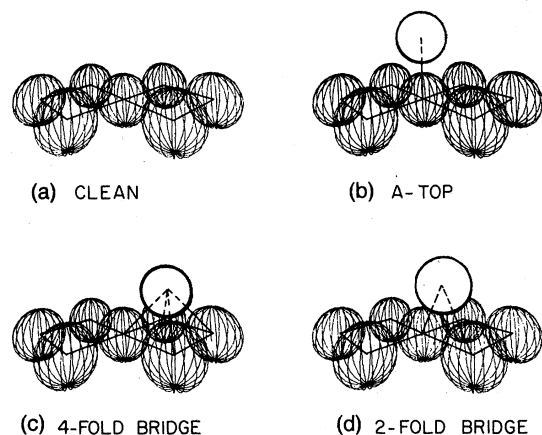(c) 4-FOLD BRIDGE   (d) 2-FOLD BRIDGE

FIG. 1. Oxygen placement on Cu(100). The open circles represent oxygen atoms and the others are copper atoms. The nearest-neighbor Cu distance is 2.54 Å. The oxygen atoms are placed at their equilibrium heights (see text).

A-TOP

2-FOLD BRIDGE

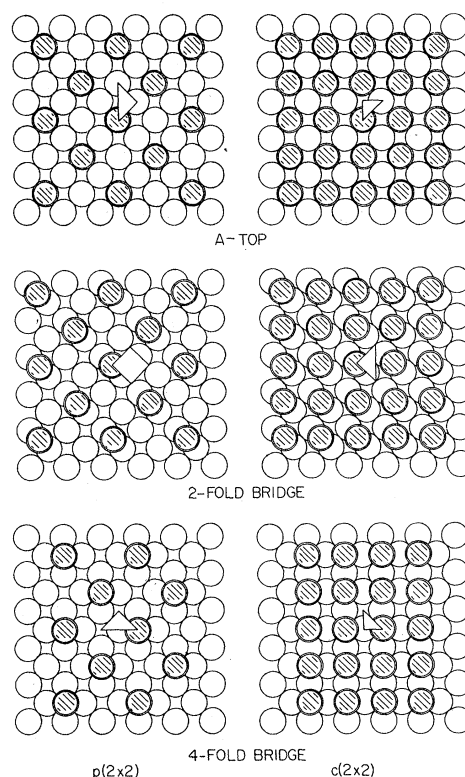4-FOLD BRIDGE

p(2×2)   c(2×2)

FIG. 2. Placement of the oxygens on the microcrystallite used in the calculations. The shaded circles represent oxygen atoms and the open circles are copper atoms. The triangles and one square are the representative impact zones for each coverage and site geometry.

tively placed on each copper atom. We have chosen the latter prescription, since it is possible to simultaneously position three or four oxygens on distant parts of the crystal to reduce the total number of impact points that need to be considered. Testing verified that our simultaneous positioning of the oxygens did not alter the oxygen ejection mechanisms or yields. Nevertheless, this single configuration required eight runs of 21 impact point sets to obtain a single yield measurement.

We have also examined the $p(2\times2)$ and $c(2\times2)$ ordered overlayer structure for the three different adsorption site geometries shown in Fig. 2. No oxygens have been placed on the edge of the microcrystallite since these positions exhibit unrealistically weak binding forces. The impact zones for all of the cases are also shown in Fig. 2; note as the symmetry decreases the size of the impact zone increases.

All trajectories reported in this work have been performed using 600-eV Ar$^+$ at normal incidence to the copper (100) surface. The microcrystallite contained four layers with 61 Cu atoms per layer, a size identical to that reported previously.[12] Considerable testing using 600-eV Ar$^+$ ion at normal incidence has shown that the number of ejected particles and the basic collision sequences are not altered by further increasing the surface area or depth of the crystallite. There are several oxygens near the crystallite boundaries that eject frequently due to the Ar$^+$ ion bombardment. These oxygens generally have low kinetic energies and do not scatter oxygens that are further from the impact point. To sample the total surface, 50–100 trajectories have been performed over the appropriate impact zone. The motion of all of the particles is

followed until the momentum of the primary ion has dissipated throughout the crystal and no more particles are found to eject. In practice we stop the calculation when the most energetic copper atom has less than 2 eV of kinetic energy, and the most energetic oxygen atom has less than 0.5 eV of kinetic energy. Choosing lower values for the stopping point does not alter the results.

The procedure used to check for multimer formation is identical to that described for the clean metals.[13,14] Briefly, after the trajectory has been stopped, we first compute for each pair of atoms i and j, the kinetic energy T_r relative to their center of mass, and their mutual potential energy V_{ij}. The potential energy V_{ij} is calculated using a Morse potential[19] which is identical in form to Eq. (3), except that it is applicable to all internuclear separations R. The gas-phase constants, as derived from spectroscopic measurements,[19,20] are given in Table I. If the total energy of the dimer

$$E_{tot}^{dimer} = T_r^{dimer} + V_{ij} \qquad (7)$$

is negative, then the tested dimer is considered to be bound. For many high yield impact points several bound dimers are formed above the surface. From these, we check for the possibility of linked or overlapping dimers. If this condition is found, the total energy of the cluster, $E_{tot}^{cluster}$, where

$$E_{tot}^{cluster} = T_r^{cluster} + \sum_{i=1}^{n-1} \sum_{j>i}^{n} V_{ij}, \qquad (8)$$

with n being the number of atoms in the cluster, is recalculated for all of the atoms in the linkage to evaluate the possibility of forming a multimer. As in the dimer analysis, if $E_{tot}^{cluster}$ for the atoms in the linkages is less than zero then the atoms are considered to be a cluster. Since exact potential surfaces are unavailable for $Cu_kO_l, k+l \geq 3$, the gas-phase dimer potentials have been arbitrarily chosen to evaluate $E_{tot}^{cluster}$. Most of the larger clusters, however, are stable even if weaker potentials are used. Thus, the mechanisms for cluster formation are valid over a wide range of conditions and do not depend on a specific choice of interaction potential.

III. RESULTS AND DISCUSSION

A. Single-atom adsorption

To gain a basic understanding of adsorbate ejection processes, we have first examined the case where a single oxygen atom is placed independently in an A-top position with $E_b = 1.32$ eV on each of the copper substrate atoms. The percentage of times that each oxygen ejects when the impact zone is bombarded at 21 different impact points by 600-eV Ar$^+$ ion at normal incidence is shown in Fig. 3. The first striking feature in Fig. 3 is that the target oxygen atom ejects the most frequently at 62% of the time. This fact is in sharp contrast to the process that occurs on clean Cu(100) where the target Cu atom is generally driven down into the solid and only ejects ~2% of the time.[12] The trajectory of the target oxygen atom, however, closely resembles the trajectory of the target copper atom on the Cu(110) face. For both of these cases, the target atom is slightly above the surface plane and is most susceptible to ejection by direct collisions with the incident ion.

We find two common pathways for oxygen atom ejection which involve direct collisions with the primary ion. The Ar$^+$ ion can strike the target oxygen atom, which subsequently reflects off a neighboring Cu atom and ejects. Alternately, the Ar$^+$ ion can initially reflect from the target copper atom, strike a nearby oxygen atom, and cause it to eject. Both direct collision mechanisms are shown schematically in Fig. 4(a).
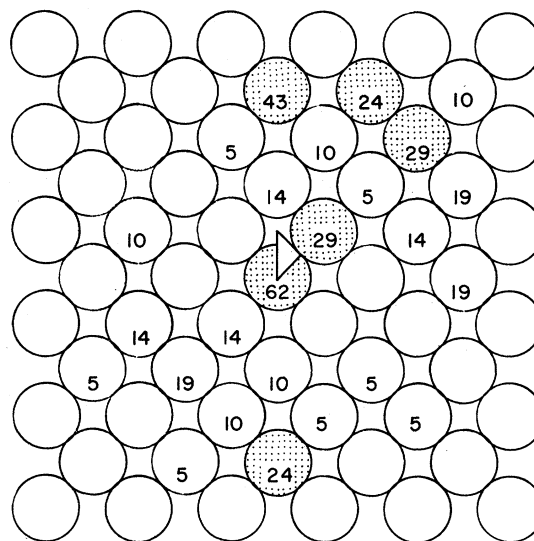
Other more complicated collision sequences can

FIG. 3. Oxygen yield for single oxygen atom adsorption. Oxygen atoms were placed independently in each of the A-top sites. The numbers are the percentage of times that the oxygen atom ejects. No number indicates that it did not eject. No oxygen atoms were placed over the outermost copper atoms as it results in artificially low E_b. The shaded atoms ejected more than 20% of the time.
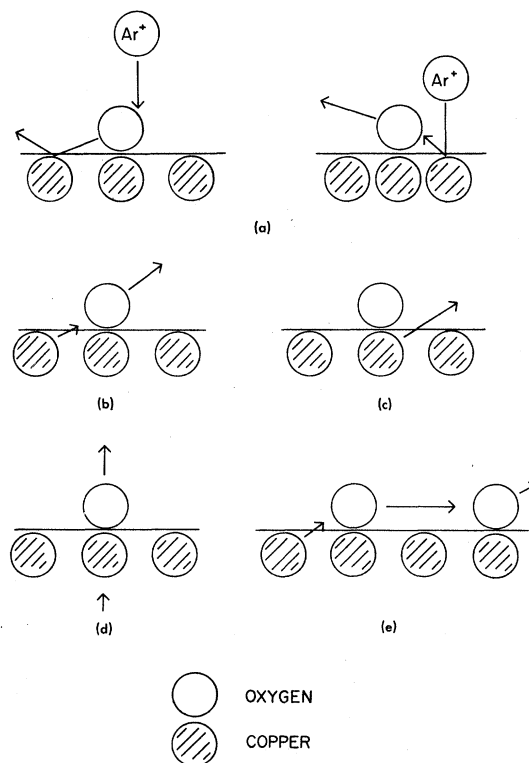
FIG. 4. Mechanisms for oxygen atom ejection on Cu(100).

be identified as important contributors to oxygen atom ejection. For example, in Fig. 4(b), the copper atom adjacent to the adsorbate starts to leave the solid, but finds an oxygen atom sticking up in its path. Depending on their collision angles and the kinetic energy of the copper atom, both particles may or may not eject. An oxygen atom can also be desorbed by the copper atom directly beneath it, as shown in Fig. 4(d), although it is more common for the copper atom to escape the solid from underneath the oxygen *without* ejecting it, as shown in Fig. 4(c). The reason for this phenomenon is that only a small percentage of the energetic copper atoms eject normally to the surface.[15]

To summarize the information given in Fig. 3, and to quantitatively illustrate how the ejection mechanisms influence the damage cross section, we have plotted the oxygen and clean copper yields versus distance from the target atom in Fig. 5. For clean Cu(100),[12] the target atom and the Ar⁺ ion move into the solid ejecting a large number of atoms which were originally about 4 Å from the target atom, as shown in curve *b* of Fig. 5. For the single atom adsorbate, this copper distribution

is not significantly altered. The target oxygen atom, as shown in curve *a* of Fig. 5, is seen to eject most frequently by the previously discussed mechanisms. Due to the large number of Cu atoms at ~4 Å that are ejecting radially outward, a large number of oxygens at ~7 Å also eject [Fig. 4(b)]. The minimum in curve *a* of Fig. 5 arises from the mechanism shown in Fig. 4(c); the copper atoms directly under the adsorbate do not generally eject atoms directly over them.

The above trajectories constitute all of the major pathways for oxygen ejection. A variety of other processes have, of course, been observed in our analysis, although most of these involve collisions between lower energy particles. These collisions usually occur late in the cascade when much of the surface structure has been destroyed. Varying E_b for oxygen on copper between 0.5 and 2.0 eV only slightly alters the fraction of particles ejecting by a specific mechanism; it does not induce the formation of any new pathways. We have reached a similar conclusion for oxygen placed in the other geometric sites on copper. Thus, having identified the major ejection mechanisms for the single adsorbed atom case, we next proceed to consider ordered overlayers at higher coverages; a regime where oxygen-oxygen collisions become probable.

B. Ordered adsorbate overlayers

The response of ordered overlayers of adsorbates to ion bombardment is computationally the most straightforward to model. They are also the easiest configurations to compare to experiment since the coverage, θ, and the ordering can be found by methods such as low-energy electron diffraction and auger electron spectroscopy. In this work, we have carefully analyzed the $p(2 \times 2)$, $\theta = 0.25$, and the $c(2 \times 2)$, $\theta = 0.50$, coverages on Cu(100). Further, the influence of varying E_b, and of altering the site geometry of the oxygen adsorbate on the ejection process has been examined quantitatively.

The effect of oxygen surface coverage and geometry on the ejection yields is shown in Table III. The first feature of these results is that, regardless of site symmetry, the oxygen yield increases by slightly more than a factor of 2 as the coverage is doubled from $p(2 \times 2)$ to $c(2 \times 2)$. This feature is noticeable for all sets of data where we have systematically varied the coverage. For the A-top configuration with E_b of 1.32 eV, for example, the oxygen yield normalized to the oxygen coverage increases by 12% and by 29% in going from the single atom case to the $p(2 \times 2)$ and $c(2 \times 2)$ coverages, respectively. Mechanistically, the dynamics show that this nonlinearity is due to scattering of oxygen atoms from other oxygen atoms, where one or both
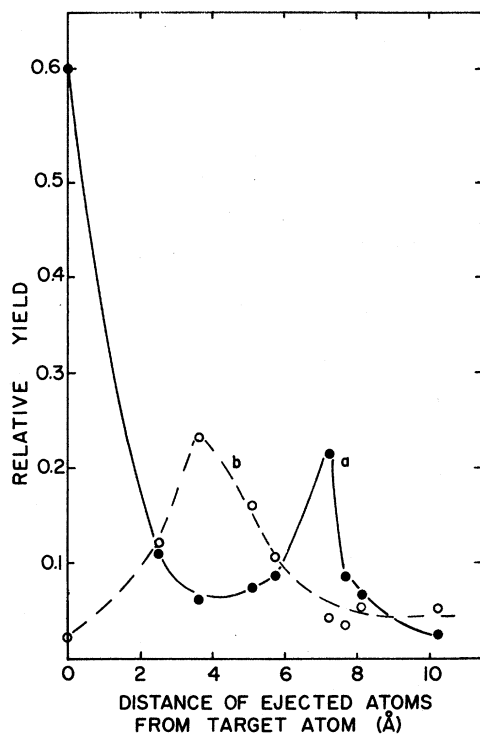

FIG. 5. Yield vs distance of ejected atoms from the target atom. Curve *a* is the relative yield for singly placed oxygen atoms in an *A*-top site on Cu(100). Curve *b* is the relative yield of copper atoms on clean Cu(100). The points represent the fraction of ejected particles per distance unit. The lines are only meant as a guide to the eye and have no physical significance.

TABLE III. Effect of surface coverage and site geometry on yields.

	Clean	A top		Fourfold bridge		Twofold bridge	
		p (2×2)	c (2×2)	p (2×2)	c (2×2)	p (2×2)	c (2×2)
E_b (eV)	•••	0.74	0.74	0.76	0.76	0.74	0.74
Number of impact points	111	66	66	110	121	110	110
Cu	436	210	191	435	416	378	331
Cu yield	3.93	3.18	2.89	3.96	3.44	3.44	3.01
O	•••	132	292	267	607	293	792
O yield	•••	2.00	4.42	2.43	5.02	2.66	7.20
Cu_2	17	7	7	20	13	11	11
O_2	•••	1	2	2	19	2	27
CuO	•••	2	7	23	34	13	33
Cu_3	3	3	0	2	2	2	1
Cu_2O	•••	1	2	0	5	3	3
CuO_2	•••	0	0	1	4	2	6
O_3	•••	0	1	0	1	0	4
Tetramers	0	1	1	1	1	0	1
Pentamers	0	0	1	0	1	1	0
Hexamers	0	0	0	0	1	0	1

may eject depending on their relative energies and the angle of impact. This sequence is an additional ejection process which becomes more prominent as the coverage increases. The mechanism is illustrated in Fig. 4(e); an oxygen can start to move away from the surface, find another oxygen in its path, and cause it to eject. The scattering chain can also be initiated by an O atom or by the primary ion itself.

We have examined the effect of E_b on yields for several of the adsorbate configurations. The yields for E_b values of 0.5, 0.74, 1.32, and 2.00 eV, reasonable values for typical chemisorption systems, are summarized in Table IV for the $c(2×2)$ A-top case. The copper yield is nearly independent of

the chosen E_b, although it is considerably lower than the yield of 3.93 atoms per ion found on the clean Cu(100) orientation.[13] The reason for this result is that the ability of the copper atoms to find their way through the overlayer depends more on where the oxygens are positioned, as we shall see in the discussion of Table III, than on how tightly the oxygen atoms are bound to the surface. The oxygen yield, on the other hand, is strongly dependent on E_b, as shown in Fig. 6. Note also that at high values of E_b the yield is leveling off due to a relatively constant number of high-energy events.
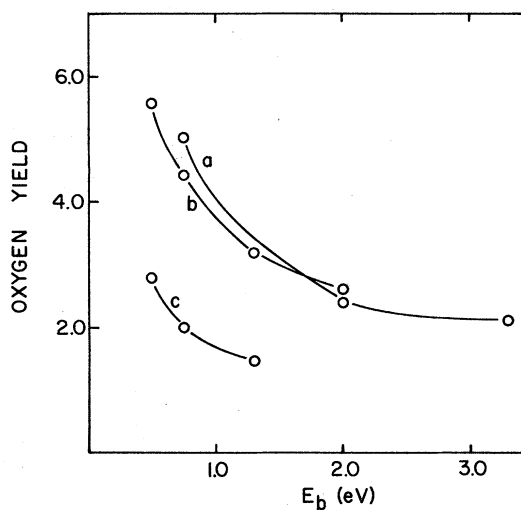
TABLE IV. Effect of E_b on yields for oxygen, c (2×2), A top.

E_b	0.50	0.74	1.32	2.00
Number of impact points	66	66	66	66
Cu	190	191	196	199
Cu yield	2.88	2.89	2.97	3.02
O	367	367	211	173
O yield	5.56	4.42	3.20	2.62
Cu_2	5	7	11	6
O_2	2	2	2	0
CuO	11	7	6	6
Cu_3	2	0	2	3
Cu_2O	3	2	2	2
CuO_2	2	0	1	0
O_3	1	1	0	0
Tetramers	2	1	1	0
Pentamers	0	1	0	0

FIG. 6. Oxygen yield vs E_b. Curve a is the c (2×2) fourfold bridge configuration, curve b is the $c(2×2)$ A-top configuration, and curve c is the $p(2×2)$ A-top configuration.

The site position exerts a strong influence on the ejection yields of both the oxygen and copper species. A summary of our calculations is shown in Table III for three site configurations and for the $p(2\times2)$ and $c(2\times2)$ coverages. For most of the cases, the copper yield decreases with increasing coverage, although to varying degrees. For the $p(2\times2)$ fourfold bridge bonded position, there is actually a slight *increase* in the copper yield relative to that of the clean Cu(100) surface. This somewhat anomalous observation arises from the fact that for the fourfold bridge geometry, the oxygen atom fills the gap in the lattice surface, effectively increasing the density of atoms available to spread the momentum of the primary ion. We have previously noted similar morphological effects.[12] The closely packed Cu(111) orientation, for example, has a particle yield 65% larger than the more open (100) face. A similar argument can be made to explain the higher copper yields when oxygen is adsorbed in a twofold bridge position relative to an A-top site.

Two major factors are then responsible for determining the magnitude of the copper yield. First, the increased density of surface atoms tends to increase the yield. Second, the oxygen overlayer physically prevents the ejection of some copper atoms by simply being in the way.

For all sites, the oxygen yield increases with increasing coverage, although not in a linear fashion due to the oxygen-oxygen scattering mechanism discussed above. Of particular note, however, is that the yield for the twofold bridge site is the largest, followed by the fourfold bridge site and the A-top site. Our analysis clearly shows that this trend arises from the mismatch in registry between the overlayer and the substrate for the twofold bridge site. The copper atoms prefer to eject along the [100] direction of the crystal— along the gaps in the lattice surface.[15] For this bridge site, however, as can be seen from Fig. 2, the ejecting copper atoms always find an oxygen atom in their path. In contrast, for the other configurations open channels exist which allow unhindered copper ejection.

The atomic copper and oxygen yield calculations point out the complexity of the processes that give rise to ejection in a multicomponent system. On the other hand, sorting out the important factors, such as the E_b and the placement of adatoms on the surface relative to the substrate, provide an important first step in elucidating the mechanism of particle ejection from ion-bombarded reacted surfaces. To complete the discussion of the atomic motion, we next consider the propensity of these species to form multimers and to relate this propensity to the structural aspects of the surface.

C. Multimer formation

From the computed trajectories presented and discussed in Secs. III A and III B we have tested for the likelihood that the ejected atoms can become part of a molecular cluster, using the prescription given in Eqs. (7) and (8). As shown in Tables III and IV many examples of multimer formation have been found with the molecules containing as many as six constituent atoms. In every case, the multimers establish their identity as clusters within interaction range of the solid. The constituent atoms do not necessarily form from contiguous atoms, but considerable rearrangement can occur. The same mechanism has been found for cluster ejection from clean copper surfaces.[13,14,18] It is not presently known, however, whether this rule will hold for molecularly adsorbed species like CO.

From the data presented in Table III, it is clear that a number of structure-sensitive factors affect multimer formation. In general, as was found for the clean metals,[13] the two closest-packed configurations give rise to the largest number of clusters. Here, the twofold bridge configuration has the largest multimer yield, since there are more oxygen atoms ejected for this geometry as discussed earlier.

In addition to the dimers and trimers reported in Table III, many larger clusters were also found including the tetramers CuO_3, Cu_2O_2, Cu_3O, and Cu_4; the pentamers Cu_2O_3 and Cu_3O_2; and the hexamers Cu_2O_4 and Cu_3O_3. Other combinations have not been detected in our calculations. A variety of metal-oxygen cluster ions have been experimentally found to be ejected from ion bombarded oxidized metal surfaces. For the $c(2\times2)$ coverage of oxygen on Ni(100), the molecular species O_2^-, NiO^-, NiO_2^-, $Ni_2O_3^-$, Ni_2^+, Ni_3^+, O_2^+, NiO^+ and Ni_2O^+ have all been detected with reasonable intensity.[6] The observation is general with analogous clusters found on W(100),[2] and most oxidized polycrystalline metal surfaces.[1]

For these particular systems, we do not predict the emission of clusters as intact parts of the solid, and the constituent atoms need not arise from contiguous points on the surface. The different points of origin for the three types of dimers found in our calculations for oxygen in a $c(2\times2)$, fourfold bridge configuration are shown in Fig. 7(a). The Cu_2 dimers arise from a fairly broad range of sites which can be as far as 6 Å apart. Nearly all of the O_2 dimers, however, originate from oxygen nearest neighbors only, 3.6 Å apart. The difference in the separation distance between O_2 and Cu_2 is due mainly to geometrical constraints inherent in their relative atomic spacings in the $c(2\times2)$ configuration. Note that for CuO, the cop-

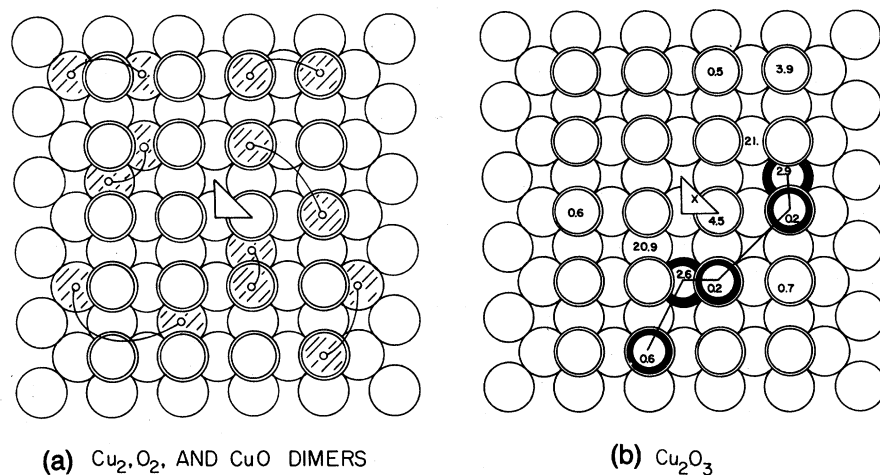**(a)** Cu_2, O_2, AND CuO DIMERS

(b) Cu_2O_3

FIG. 7. Point of origin of molecular clusters. The double circles represent oxygen atoms and the single circles are copper atoms. Frame (a) shows typical Cu_2, O_2, and CuO dimers. The placement on the crystal surface is arbitrary. Frame (b) shows the Cu_2O_3 pentamer. The numbers are the kinetic energies (eV) of the ejected atoms. The **×** is the impact point that yields this pentamer.

per and oxygen atoms originate from only nearest-neighbor and next-nearest-neighbor positions, intermediate between that of Cu_2 and O_2.

Many larger clusters are also found in our calculations. As is true for the case of clean metals,[14] the clusters tend to originate from a localized region of the surface. In fact, for the copper-oxygen system, all multimers can be encompassed by a circular region of radius of roughly 5 Å. As the clusters get larger, they tend to retain more of the local atomic structure of the surface. Most trimers, for example, contain at least one pair of atoms that originated from nearest neighbors. The constituent atoms of the cluster, Cu_2O_3, are shown in Fig. 7(b) and are quite typical of the location of the atoms that comprise the larger species. The kinetic energies of the atoms as they leave the surface are also shown in the figure. As was pointed out in our previous discussions of cluster formation,[13,14] the energies of the atoms in the cluster tend to be rather small since all of the particles need to be above the surface at approximately the same time.

The local surface structure and coverage are strongly reflected in the multimer yields that are reported in Tables III and IV. The first point is that the number of Cu_2 and Cu_3 species does not decrease significantly as the surface coverage is increased to 0.5 monolayer of oxygen. Our analysis shows that the reason for this result is that the number of slower moving ejecting copper atoms, which are the ones that most easily form multimers, is not significantly lower. The probability of dimer and trimer formation is therefore not significantly altered. Experimentally, large Ni_2^+ and measureable Ni_3^+ ion intensities have been measured for the $c(2 \times 2)$ oxygen covered Ni(100) surface.[6] It is not until the formation of a bulk NiO

species that the trimers are observed to disappear, partly due to the increased distance between Ni atoms in the surface layer.

The O_2 formation probabilities are strongly influenced by surface structure. Note that in Table III, the O_2 yield is nearly ten times higher for the $c(2 \times 2)$ bridged configurations than for the equivalent $p(2 \times 2)$ configurations. This result is simply a manifestation of the larger O-O separation distance for the lower coverages. A similar argument can be used to tentatively explain the CuO_2 and O_3 trimer yields. The experiments on Ni(100) again corroborate these predictions in that the O_2^- to O^- intensity ratio is observed to increase by a factor of 4 in going from $p(2 \times 2)$ to $c(2 \times 2)$ and the NiO_2^- to NiO^- ratio exhibits a strong increase with coverage until the bulk NiO starts to form. We take ratios to compare to our calculations since the uncertain effects of ionization probability on the ion yield will be minimized. Much lower O_2 yields are calculated when the oxygens are in A-top positions, and when E_b is increased, due mostly to the lower oxygen atom yield. For the $c(2 \times 2)$ twofold bridged position, for example, the number of O_2 species drops from 27 to 6 as E_b is increased from 0.74 to 1.97 eV.

Systematic trends are also observable for the CuO yields. The most important observation is that the calculated number of CuO molecules decreases with increasing E_b, a result opposite to what one might expect for molecular CuO ejection. The reason for this trend is that when E_b is low, the oxygen yield is high, increasing the chance for CuO formation over the surface. The CuO yield roughly increases with oxygen coverage, being considerably higher for the bridged geometries. The higher CuO yield in this case is also due to the increased number of ejected oxygen atoms.

D. O_2^- and O_2^+ formation

For the specific case of molecular oxygen forma-
tion, we are able to examine the effect of charge
state on the dimer formation probabilities since the
Morse potential parameters can be determined for
O_2^+ and O_2^-.[19,20] By putting these parameters into
Eq. (3) and using the criteria for dimer formation
in Eq. (7), the probability of forming a dimer be-
tween an O^- or O^+ ion and an O atom can be de-
duced. The results of this calculation are summa-
rized in Table V for oxygen in a $c(2 \times 2)$ coverage.

Varying the O_2 charge state alters the number of
dimers to some degree, although the normalized
yields change by less than a factor of 2, even con-
sidering the rather poor statistics. The most
striking feature of these results, however, is that
the thermodynamically most stable species, O_2^+,
produces the *lowest* number of dimers. The reason
for this fact is that the range of the potential is the
smallest for this species. Apparently the number
of possible two-body interactions that a particular
atom might experience is more important than the
ultimate stability of a dimer in its equilibrium con-
figuration.

This calculation is of particular interest since it
gives a rough idea of how much the dimer yields
are perturbed by ionization, and of how sensitive
the relative yields are to changes in the potential
function. The data in Table V clearly show that
many of the conclusions we have made concerning
the formation of neutral molecules may be applic-
able to the formation of molecular ions as well.

IV. CONCLUSION

We believe that modeling the response of reacted
single-crystal surfaces to ion bombardment by
classical dynamics provides unique insight into the
atomic motion that gives rise to particle formation.
As we have shown, to interpret the macroscopic
observables one must understand the detailed pro-
cesses going on inside the crystal. The fact that
the oxygen-oxygen scattering induces a nonlinearity
in the O atom yield with coverage is an example.
In fact, for these multicomponent systems, it is
clear that the full dynamics must be included or
important processes can be overlooked.

In this study we have presented a detailed investi-
gation of how adsorbed atoms are ejected from
metal surfaces. Probably the most important con-
clusion is that the atomic placement and crystal
structure exert a strong influence on atomic and
molecular ejection, which is explainable only after
examination of the actual dynamics. For example,
the oxygens in the twofold bridge position eject
most frequently since their slightly off-line position
puts them in the way of more ejecting copper
atoms. The enhanced oxygen atom yield is also
partly responsible for the enchanced multimer
yield for this configuration. A second main conclu-
sion is that the clusters establish their identity
over the surface and do not necessarily form from
contiguous surface atoms. The rearrangement is
somewhat predictable in that the atoms do arise
from a localized region of the surface of radius of
roughly 5 Å.

TABLE V. Effect of charge state on O_2 formation[a].

	A top	Fourfold bridge	Twofold bridge
E_b eV	0.74	0.76	0.74
Number of trajectories	66	121	110
Species [b]			
O_2^-			
Monomers	268	477	622
Dimers	5	29	39
Dimer yield [c]	1.0	3.2	4.7
O_2			
Monomers	274	510	671
Dimers	2	19	27
Dimer yield [c]	1.0	5.2	8.1
O_2^+			
Monomers	277	512	689
Dimers	2	18	18
Dimer yield [c]	1.0	4.9	5.4

[a] Coverage is $c(2 \times 2)$ in all cases.
[b] Potential parameters are given in Table I.
[c] Normalized to the A-top case.

These calculations establish most of the key elements involved in the ejection of atoms and molecules from the copper-oxygen model system. The main limitation of this approach is, of course, that except for our example of O_2^+ and O_2^- ejection, the surface ionization is not included directly, and it is generally these ions which are detected experimentally. It is hoped, however, that a detailed knowledge of the solid motion on an atomic level can lead to equally sophisticated theories of the ionization event.

ACKNOWLEDGMENTS

*Present address: Dept. of Chemistry, Purdue Univ., West Lafayette, Ind. 47907.

[1] A. Benninghoven, Surf. Sci. 35, 427 (1973).

[2] M. L. Yu, Surf. Sci. 71, 121 (1978).

[3] M. Barber, J. C. Vickerman, and J. Wolstenholine, J. Chem. Soc. Faraday Trans. I 72, 40 (1976).

[4] P. H. Dawson, Phys. Rev. B 15, 5522 (1977).

[5] E. Taglauer, G. Marin, W. Heiland, and U. Beitat, Surf. Sci. 63, 507 (1977).

[6] T. Fleisch, N. Winograd, and W. N. Delgass, Surf. Sci (to be published).

[7] M. Barber, J. C. Vickerman, and J. Wolstenholme, Surf. Sci. 37, 68 (1977).

[8] H. F. Winters and P. Sigmund, J. Appl. Phys. 45, 4760 (1974).

[9] E. Taglauer, U. Beitat, and W. Heiland, Third International Conference on Ion Beam Analysis Proceedings, Washington, D. C., 1977 (unpublished).

[10] P. Williams and C. A. Evans, Jr., Appl. Phys. Lett. 30, 559 (1977).

[11] M. L. Yu, Phys. Rev. Lett. 40, 574 (1978).

[12] D. E. Harrison, Jr., P. W. Kelly, B. J. Garrison, and N. Winograd, Surf. Sci. 76, 311 (1978).

[13] N. Winograd, D. E. Harrison, Jr., and B. J. Garrison, Surf. Sci. 78, 0000 (1978).

[14] B. J. Garrison, N. Winograd, and D. E. Harrison, Jr., J. Chem. Phys. 69, 1440 (1978).

[15] N. Winograd, B. J. Garrison, and D. E. Harrison, Jr., Phys. Rev. Lett. 41, 1120 (1978).

[16] D. E. Harrison, Jr., N. S. Levy, J. P. Johnson, III, and H. M. Effron, J. Appl. Phys. 39, 3742 (1968).

[17] D. E. Harrison, Jr., W. L. Moore, Jr., and H. T. Holcombe, Radiat. Eff. 17, 167 (1973).

[18] D. E. Harrison, Jr. and C. B. Delaplain, J. Appl. Phys. 47, 2252 (1976).

[19] G. Hertzberg, Molecular Spectra in Molecular Structure I. Spectra of Diatomic Molecules (Van Nostrand, New York, 1950).

[20] B. Rosen, International Tables of Selected Constants (Pergamon, New York, 1970).